Optimal Rehabilitation of Gas Distribution Pipelines in Liquefiable Soils Considering Seismic Reliability

Vindhyawasini Prasad, S.M.ASCE[1]; and Kalyan R. Piratla, A.M.ASCE[2]

Abstract: Continuous functioning of gas distribution networks (GDNs) is important in the aftermath of an earthquake. Liquefaction has been found to cause a majority of the damages to buried pipeline infrastructure during an earthquake. A model for quantifying the seismic reliability of city-level GDNs is presented in this study. The seismic reliability model was used to select optimal rehabilitation alternatives for buried gas pipelines. Cured-in-place lining (CIPL) and replacement of aging pipelines with high-density polyethylene (HDPE) pipelines using the pipe bursting method were considered as rehabilitation alternatives in the study. A synthetic GDN was designed appropriately using the land-use pattern of the peninsular region of Charleston, South Carolina for demonstration purposes, and the 1886 Charleston earthquake was selected as the representative seismic hazard. Serviceability of the GDN was adopted as the basis for the reliability assessment using the Monte Carlo simulation approach, and a computationally efficient gas-flow model was developed to quantify the serviceability. For the selected seismic hazard, the reliability of the GDN in the study area was found to be 16.78%, and it increased to 18.62% after CIPL lining of all the pipelines. Replacement of all aging pipes with HDPE increased the reliability further to 26.94%. The optimization results informed the optimal selection of the rehabilitation alternative for each pipeline to maximize seismic reliability of the GDN at the cheapest possible cost. The proposed seismic reliability assessment approach and its use for rehabilitation planning will aid gas pipeline operators in their capital improvement works. **DOI: 10.1061/(ASCE)PS.1949-1204.0000545.**

Author keywords: Liquefaction potential; Seismic reliability; Monte Carlo simulations.

Introduction

Gas distribution networks (GDNs) play an important role in ensuring energy security to communities. Their importance has increased in recent decades due to the (1) falling price of natural gas, and (2) increased adoption of and reliance on distributed gas-based power generation units. Gas-based power generation units are especially important in the aftermath of hazards such as earthquakes when the traditional grid-based electricity supply is likely to be interrupted. The GDNs themselves are vulnerable to earthquakes because they critically are served by buried pipelines. Given the uncertainties associated with determining the condition of aged gas pipelines and their resulting vulnerability to various seismic hazards, it is important for energy utilities to have a strategic framework for enhancing the seismic reliability of their systems as part of capital improvement planning. This study presents a seismic reliability assessment framework using the Monte Carlo simulation (MCS) technique for GDNs and used it to determine optimal rehabilitation strategies for a chosen study area.

Seismic reliability of GDNs has been investigated in recent years through studies varying in approach and scale of the networks considered. One of the first studies of seismic reliability of city-level GDNs was that by Cret et al. (1993). They conceptualized a damage estimation model considering residential blocks as the consumer nodes. The main optimization parameter used in their work was the control of shut-off valves using fuzzy set theory. The performance of a real-world network during a 6.7-magnitude earthquake in Tokyo city was used to validate their model. They did not consider updating the infrastructure, but focused completely on the operational aspects. A detailed literature review of the performance of buried natural gas pipelines was compiled by Psyrras and Sextos (2018), focusing on the modes of failure and investigating the effects arising from ground shaking.

In an experimental study, Miao et al. (2016) tested a small, representative buried-pipeline network. The development of strains in the steel pipelines was analyzed for a seismic event mimicked by the use of trinitrotoluene (TNT) explosive. The axial strains were found to be larger than the bending strains. They did not study the effect of permanent ground deformations (PGDs), but focused only on transient ground deformations (TGDs). In the present study, the emphasis was more on liquefaction-induced PGDs. Landslides are the other type of PGD observed during seismic activity. Impacts of landslides on the buried gas pipelines were investigated by Yiğit et al. (2017). They analyzed the behavior of gas transmission pipelines passing through an earthquake-prone region near the North Anatolian Fault Zone in Turkey.

A useful simulation technique often used in reliability assessment studies on lifeline systems is the Monte Carlo simulation technique (Ameri and van de Lindt 2019; Liu et al. 2017; Nuti et al. 2010; Praks et al. 2017; Stern et al. 2017). Nuti et al. (2010) studied the performance of electricity, water, and road networks during an earthquake using MCS and simulation of flow in different networks without considering the interdependencies among the networks. Praks et al. (2017) used a MCS-based method to quantify the vulnerability of a real-world gas transmission network due to the failure of random components. Liu et al. (2018) validated a probability density evolution method for the reliability assessment of gas networks using MCS. Ameri and van de Lindt (2019) used MCS to

[1]Formerly, Graduate Research Assistant, Glenn Dept. of Civil Engineering, Clemson Univ., Clemson, SC 29634. ORCID: https://orcid.org/0000-0003-0585-7217. Email: vindhyp@g.clemson.edu

[2]Liles Associate Professor, Glenn Dept. of Civil Engineering, Clemson Univ., Clemson, SC 29634 (corresponding author). ORCID: https://orcid.org/0000-0003-0836-7598. Email: kpiratl@clemson.edu

Note. This manuscript was submitted on January 21, 2020; approved on November 19, 2020; published online on March 24, 2021. Discussion period open until August 24, 2021; separate discussions must be submitted for individual papers. This paper is part of the ***Journal of Pipeline Systems Engineering and Practice***, © ASCE, ISSN 1949-1190.

evaluate and compare the restoration time in the aftermath of an earthquake for GDNs with high-density polyethylene (HDPE) and steel pipelines. Liquefaction was considered as the hazard in their study, but the reliability was evaluated purely based on topological connectivity-based metric. They evaluated the fragility of steel pipelines using empirical relations, but assumed no breakage for HDPE pipelines, a potential limitation which was addressed in the present study. The comparison of the performance of steel and HDPE pipelines lacks adequate analysis in the literature possibly due to the absence of past damage data for HDPE pipelines. Prasad et al. (2020) developed a model to evaluate the seismic reliability of GDNs. The same model was extended in the present study to evaluate the reliability improvement with different pipeline renewal options using an optimization framework. Recent advancements in the area of pipeline rehabilitation have helped utilities to find solutions for the issues associated with aging pipeline infrastructure. This study highlighted the relevance of seismic reliability as an important measure for pipeline rehabilitation planning in seismically active regions. The obligation to rehabilitate aging infrastructure can be seen as an opportunity to strengthen its seismic performance.

Many previous studies of seismic reliability assessment that relied on fragility relations of components have used connectivity-based serviceability metrics (Poljanšek et al. 2012). Flow-based models have been used to model random failures and their impact on network reliability (Praks et al. 2017), but they rarely have been used to investigate the seismic reliability of GDNs. This study filled this gap by using a combination of empirical relations and limit state analyses in conjunction with a flow-based reliability assessment model to develop a framework for optimizing the rehabilitation of GDNs. The proposed framework uses seismic reliability as the objective in the optimization process for rehabilitation planning. The objective of this study was to present and demonstrate a strategic seismic reliability improvement framework for GDNs through pipeline rehabilitation planning. The framework was demonstrated on a hypothetical, representative gas distribution network made of cast iron (CI) pipelines. Three different rehabilitation options were explored: cured-in-place lining (CIPL), replacement with HDPE pipeline of the same diameter, and replacement with HDPE pipeline of a larger diameter. The study (1) formulated a Monte Carlo simulation–based seismic reliability assessment framework including adapting fragility equations for different pipeline materials considered, (2) developed a hypothetical and yet representative GDN for an urban area prone to seismic hazards, (3) characterized relevant seismic hazards for the study area of interest, and (4) demonstrated the seismic reliability improvement framework using the chosen study area.

Methodology

This section describes the approaches adopted to assess the seismic reliability of GDNs and the characterization of the seismic hazard considered in the study.

Design of Study Area GDN

Because of the lack of real-world data, which are difficult to obtain, a hypothetical GDN made of cast iron pipelines was designed for a chosen study area in Charleston, South Carolina. The network comprised high-pressure distribution mains with maximum allowable operating pressure (MAOP) of 689.476 kPa (gauge) (100 psig), medium-pressure service lines with MAOP of 310.264 kPa (gauge) (45 psig), and regulator stations which connect pipelines operating at two different pressure ratings. The network consisted of pipelines of various diameters, ranging from 76.2 mm (3 in.) to 762 mm (30 in.). Service laterals were not considered a part of the network to avoid a cumbersome network topology. The layout of the network was finalized along the major streets first. The demand at the nodes was determined based on the data available in the operation reports from the real-world network operating in the region (Dominion Energy 2018). A gas flow model called the linear pressure analog (LPA) was used to simulate the gas flow in the network by solving generalized gas flow equations [Eq. (1)] simultaneously for all the links in the network. The simulation of the gas flow was ensured by the use of LPA, which reduces the computational cost of the simulations significantly (Ayala H and Leong 2013)

$$Q_i = C\frac{1}{\sqrt{f_i}}\frac{T_n}{P_n}\frac{d_i^{2.5}}{\sqrt{Sl_iTZ}}\left((p_1^2 - p_2^2) - k\frac{p_{av}h_i}{ZT}\right)^{0.5} \quad (1)$$

where subscript i denotes index for links in network; Q_i = gas discharge; d_i = diameter; l_i = length; f_i = friction factor; h_i = elevation difference across pipeline; p_1 and p_2 = pressure at inlet and outlet of pipe, respectively; S, T, and Z = specific gravity, temperature, and compressibility factor of gas, respectively; and T_n and P_n = temperature and pressure, respectively, at standard conditions. The friction factor was computed using

$$\frac{1}{\sqrt{f_i}} = 4.0\log_{10}\left(\frac{3.7d_i}{e_i}\right) \quad (2)$$

where e_i = pipe roughness. Eqs. (1) and (2) were solved iteratively in tandem with a genetic algorithm optimization framework to design a hypothetical representative GDN which consisted of 443 pipelines, 16 regulator stations, 1 city gate station, 3 power generation units, and 235 demand nodes. The objectives of the design were to minimize installation costs while meeting the required nodal demands. The same flow model, based on Eqs. (1) and (2), was used to simulate the hydraulics of gas flow in the network during the optimization for rehabilitation planning. The final benchmark network is depicted in Fig. 1.

Reliability Model

A serviceability-based reliability model was used in this study. The model used Monte Carlo simulations and basic concepts of graph theory to assess the reliability of a GDN. Fig. 2 illustrates the workflow of the reliability model framework. The illustrated framework was used to evaluate the reliability of GDNs as the fraction of demand satisfied in the aftermath of the representative seismic hazard.

In the MCS, all the pipelines (i) were assigned a random number ranging from 0 to 1 as the probability of failure (R_f). The random probability of failure was compared with the fragility of the corresponding pipeline (P_f), which was evaluated using the fragility model in each iteration (N) of the MCS; P_f and R_f were arrays with N_L elements, where N_L is the number of pipelines in the network. Each element in R_f was compared with the corresponding term in P_f. Pipelines with random probability of failure exceeding the calculated fragility were considered to be failed, and the network was updated after removing those pipes. Flow simulation of the updated network gave value of the reliability index (RI_N) for one iteration. The average of the reliability index converged as the number of iterations increased. Fig. 3 shows the convergence of reliability metric as the number of iterations increased in the MCS. The dashed-dotted lines show the bounds of $\pm 2.5\%$, which was used as the convergence criteria in the MCS. The convergence for $\pm 2.5\%$ was achieved with 1,000 iterations (Fig. 3). Therefore, only 1,000 iterations were used wherever MCS was used in this study.

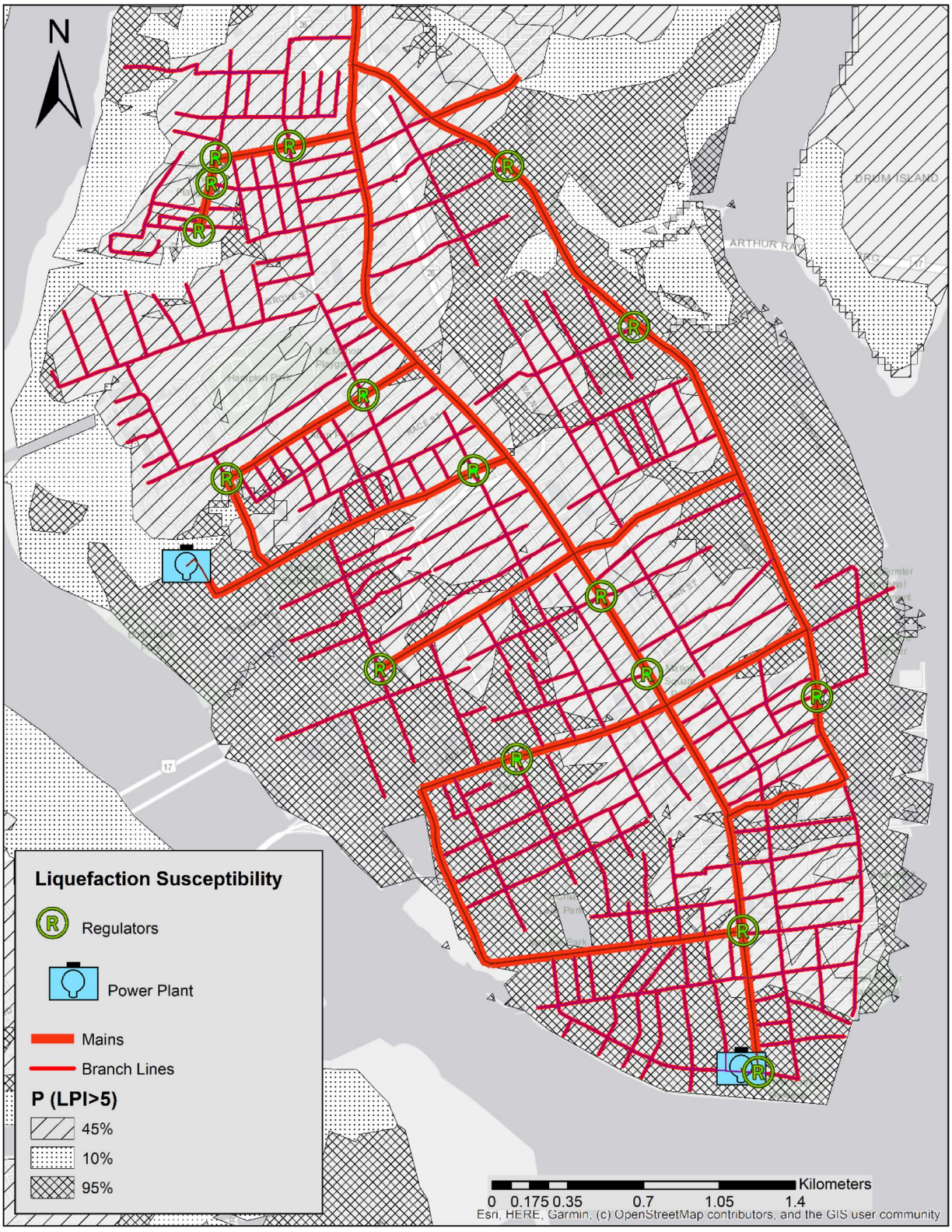

Fig. 1. Layout of the hypothetical gas distribution network designed for the study area. (Reprinted from Prasad et al. 2020, © ASCE; base map by Esri, HERE, Garmin, © OpenStreetMap contributors, and the GIS user community.)

Hazard Characterization

The 1886 Charleston earthquake was considered as the seismic hazard scenario in this study. The epicenter of the earthquake was about 30 km northeast of the peninsula, near the Woodstock fault. Peak ground acceleration of $0.3g$ and peak ground velocity of $0.49\ \mathrm{m/s}$ were used as intensity measure (Farahmandfar et al. 2016; Hayati and Andrus 2008). Permanent ground deformations can occur during an earthquake in the form of fault movement, landslide, settlement, and liquefaction. Because the study area does

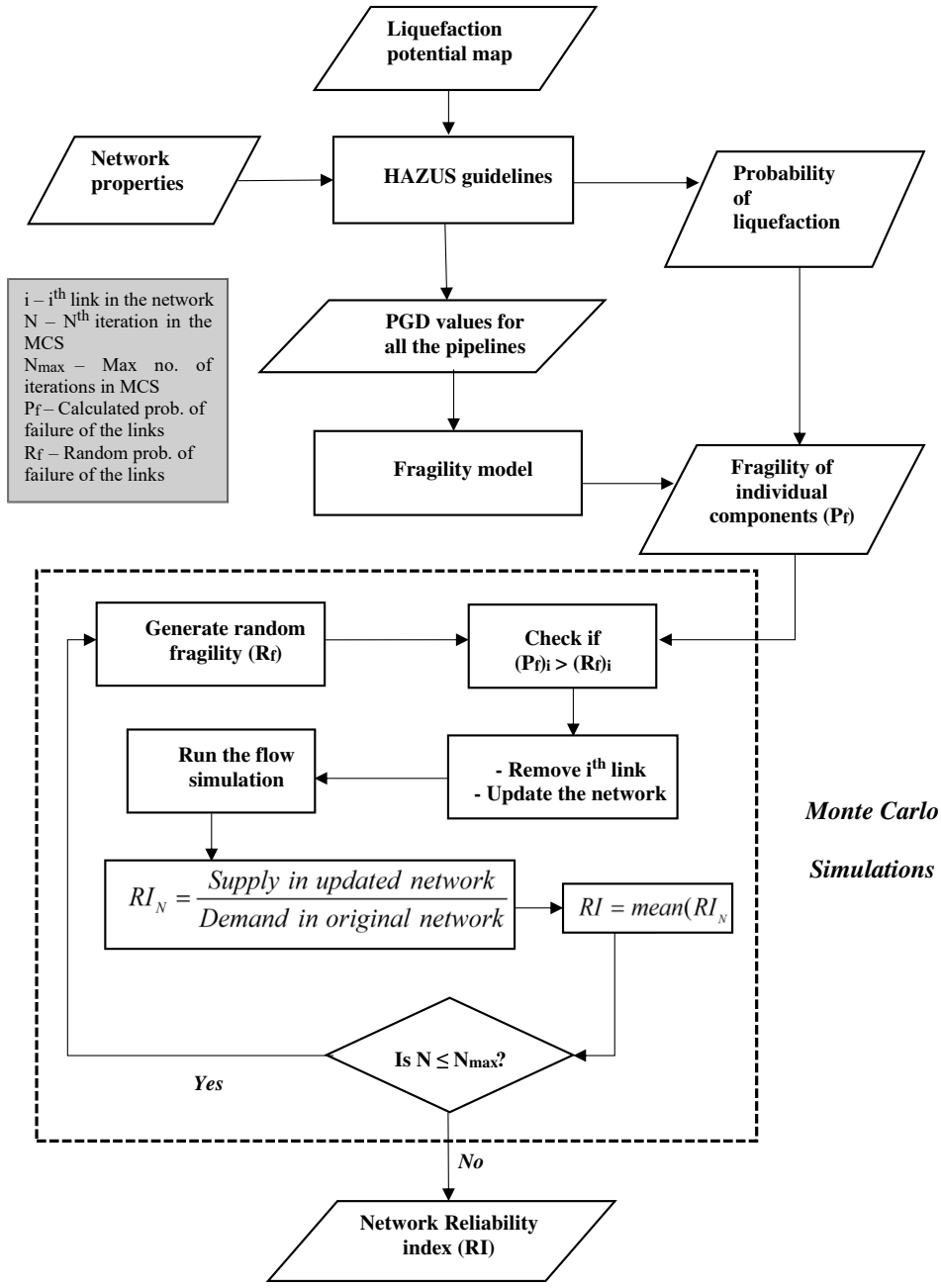

Fig. 2. Seismic reliability framework. (Adapted from Prasad et al. 2020.)

not contain any fault plane, PGDs due to fault movements were not considered in this study. Liquefaction and settlement were the observed forms of PGD during the 1886 Charleston earthquake, per several first-hand records summarized by Hayati and Andrus (2008). A liquefaction map of the study area was developed by Elton and Hadj-Hamou (1990) based on standard penetration tests (SPTs). Liquefaction potential index (LPI) is a widely used index to quantify the vulnerability of a region to liquefaction. Soils with LPI < 5 are verified to have low vulnerability to liquefaction (Iwasaki et al. 1984); therefore, LPI > 5 was selected as the cutoff value in the preparation of the liquefaction potential map for the study area (Hayati and Andrus 2008). The map is based on cone penetration tests (CPTs) conducted at 44 different locations across the study area. The map developed by Hayati and Andrus (2008) also used the previously available SPT-based liquefaction map, first-hand evidence of liquefaction during the 1886 earthquake, and the geology of the region. The liquefaction potential map developed by Hayati and Andrus (2008) categorized the study area into three zones of liquefaction potential index (LPI) > 5: (1) <10% probability, (2) 45% probability, and (3) 95% probability. The liquefaction potential map and the layout of the GDN in the study area are presented in Fig. 1. Probability of liquefaction (P_{liq}), lateral spread, and settlement values for all the GDN pipelines were calculated using the methodology presented in the Hazus-MH loss assessment model (FEMA 2012). Resultant PGD values were calculated as the vector sum of lateral spread and settlement for all the pipelines in three different zones (Table 1).

Fragility of Pipelines Made of Different Materials

Pipelines of different materials behave differently during ground shaking and permanent ground movements. This study encompassed

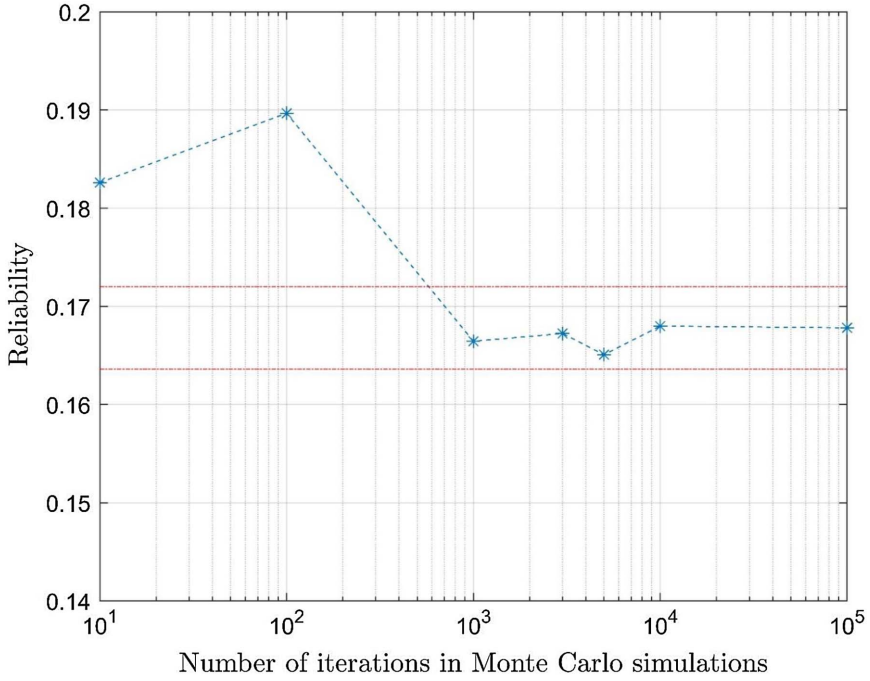

Fig. 3. Convergence of seismic reliability in the Monte Carlo simulation within ±2.5% of the converged value.

Table 1. Values of PGD for regions with different liquefaction susceptibility

P(LPI > 5) (%)	Probability of liquefaction (P_{liq})	Lateral spread (mm)	Settlement (mm)	PGD (mm)
10	0.009	130.56	25.4	133.10
45	0.088	304.8	50.8	309.12
95	0.421	1,354.58	304.8	1,388.62

GDNs consisting of cast iron, cast iron pipes lined with CIPL, and HDPE pipes. Fragility was defined as the probability of failure of a particular pipeline segment during the occurrence of the selected seismic hazard.

CI Pipe

Fragility of existing CI pipes was calculated using the empirical fragility curves in ALA (2001). The fragility functions are given in terms of repair rate (RR), i.e., the number of breaks per kilometer for buried pipelines. Repair rates were calculated using the values of PGD. Fragility induced by transient ground deformation can be calculated using peak ground velocity (PGV) as the intensity measure of the earthquake. The relations for the calculation of repair rate are presented in Eqs. (3) and (4) (ALA 2001). These also are called backbone relations for pipeline fragility estimation. The backbone curves are used to calculate the fragility of different materials after adjusting them for the pipe materials and pipe sizes. The corresponding coefficients are adapted from ALA (2001)

$$\mathrm{RR}_{\mathrm{TGD}} = K_1 K_t \cdot 0.00241 \cdot \mathrm{PGV} \tag{3}$$

$$\mathrm{RR}_{\mathrm{PGD}} = K_2 K_t \cdot 2.58 \cdot \mathrm{PGD}^{0.319} \tag{4}$$

where PGV = peak ground velocity (cm/s); PGD = permanent ground deformation (cm); K_1 and K_2 = correction factors to be used for adjustment of pipe material and pipe size subject to TGD and PGD, respectively; K_t = correction factor for adjustment of condition of pipeline (Farahmandfar et al. 2016); and RR = number of breaks per kilometer

$$\mathrm{RR} = \mathrm{RR}_{\mathrm{PGD}} \cdot P_{\mathrm{liq}} + \mathrm{RR}_{\mathrm{TGD}} \cdot (1 - P_{\mathrm{liq}}) \tag{5}$$

where RR = net repair rate considering combined effect of TGD and PGD (Farahmandfar et al. 2016); and P_{liq} = probability of liquefaction (Table 1).

For CI pipes with rubber gasket–type joints, $K_1 = 0.8$ and $K_2 = 0.8$ (ALA 2001). A value of $K_t = 1$ was assumed in this study (Farahmandfar et al. 2016). A Poisson distribution was assumed for pipe breaks to estimate the failure probability (Farahmandfar et al. 2016; Tchórzewska-Cieślak et al. 2018). Considering the occurrence of at least one break as the failure of the particular pipe, the probability of failure can be calculated as

$$P_{fi} = 1 - e^{-\mathrm{RR}_i L_i} \tag{6}$$

where P_{fj} = probability of failure of ith pipe; L_i = length of ith pipe (km); and RR_i = repair rate of ith pipe (breaks/km).

CIPL-Lined CI Pipes

Cured-in-place lining systems are used for trenchless rehabilitation of mainly cast iron and steel pipelines in gas systems. CIPL consists of three components—elastomers, adhesive, and fabric. CIPL was considered for the rehabilitation of GDN pipelines in this study as a way to extend their useful life without completely replacing them. The CIPL under consideration was tested extensively for lap strength and peel strength of the liner using a combination of field-aging and 100-year-equivalent mechanical aging in a laboratory, and the results indicated that aging did not significantly impact the strength of the CIPL (Stewart et al. 2015). The properties of CIPL differ from conventional cured-in-place pipe (CIPP) mainly in terms of the higher flexibility and impermeable elastomer barrier that makes it capable of preventing the gas from escaping. Due to lack of empirical data on failure of lined CI pipes, an experimental study on CIPL-lined ductile iron (DI) pipelines was conducted by Argyrou et al. (2018) considering the DI pipes as a proxy for

CI pipes with weak joints. In addition, properties of CIPL-lined CI pipes were studied by Netravali et al. (2003). The results of Argyrou et al. (2018) were adapted in this study to evaluate the probability of failure considering joint failures. Probability of joint failure was defined as the ratio of displacement at joints to critical joint-displacement values at pipe failure. Joints are one of the weakest spots in segmented pipelines, and a majority of breaks during earthquakes occur at joints in the form of axial pull-out and bell crushing (Ayala and O'Rourke 1989; Elhmadi and O'Rourke 1990; Housner and Jennings 1972). Considering these factors, axial pull-out was given a significant weightage in calculation of the fragility

$$P_{\text{axial}} = \frac{d_{\text{axial}}}{d_{\text{rupture}}} \tag{7}$$

where d_{axial} = joint displacement induced by PGD during earthquake; and d_{rupture} = joint displacement at rupture of the liner in the experimental study.

Calculation of displacement is based on the ground strain given for segmented pipelines during permanent deformations (O'Rourke and Nordberg 1992)

$$d_{\text{axial}} = \alpha \cdot l \tag{8}$$

where l = length of pipe segment between two joints, and this study assumed 6.1-m-long (20 ft) pipe sections for cast iron pipes; and α = ground strain, which was calculated using the following relation (O'Rourke and Nordberg 1992):

$$\alpha = \frac{\delta_{\text{axial}}}{L} \tag{9}$$

where δ_{axial} = PGD (Table 1); and L = length of PGD zone.

An assumption was made in the calculation of ground strain regarding the direction of PGD. Because PGD values lack any information about the direction of the ground movement, the direction of PGD was assumed to be at an inclination of 45° from the axis of the pipe. This assumption was made to average out the effect of the PGDs in different directions

$$\delta_{\text{axial}} = \text{PGD} \cdot \cos(45°) \tag{10}$$

The results of the axial pull-out tests were representative of the longitudinal failure of the pipes occurring at the joints, which is a common mode of failure (Singhal and Benavides 1983). Damage to pipelines in 2004 Niigata Ken Chuetsu earthquake in Japan was studied by Scawthorn et al. (2006). They compiled a database of damages in lifeline systems. One of the major findings was that a majority of the CI pipelines failed at the joints. The other failure modes, e.g., flexural cracks, are not represented by displacement-based fragility formulation assumed so far. To address these uncertainties, only a portion of fragility was assumed to be imparted by the joint failures

$$P_f = (P_f)_{\text{axial}} \cdot w_{\text{axial}} + (P_f)_{\text{ALA}} \cdot (1 - w_{\text{axial}}) \tag{11}$$

where $(P_f)_{\text{axial}}$ = probability of failure of liner at joint due to axial forces; w_{axial} = component of fragility from axial failure, i.e., due to failure of liner; and $(P_f)_{\text{ALA}}$ = pipe fragility calculated using fragility curve for PGD (ALA 2001).

Based on the discussion in Scawthorn et al. (2006) and Singhal and Benavides (1983), it can be concluded that axial failure is the prevalent mode of failure in segmented CI pipes. A conservative assumption was made by keeping w_{axial} equal to 0.5 in this study. In other words, only half of the failures were considered to be in the form of axial pull-out. For lined CI pipes, the focus solely was on improving the performance of the joints during the earthquakes. Therefore, failures arising due to reasons other than joint failures have been considered unchanged even after the application of CIPL as given in Eq. (11).

HDPE Pipes

HDPE pipelines were analyzed considering a continuous (i.e., fused) pipeline system with no significance given to the vulnerability of joints. Due to lack of adequate empirical relations for the damage of HDPE pipelines, simple analytical loading equations were used to calculate the loading on HDPE pipelines and the resulting strain values. Soil–pipe interaction was used for three components: (1) axial, (2) transverse horizontal, and (3) transverse vertical (ASCE 1984). Ramberg–Osgood equations were used to estimate the nonlinear portion of the stress–strain curve near the yielding points for continuous metallic pipes in some recent studies (Chenna et al. 2014; Nakai and Yokoyama 2015; Ramberg and Osgood 1943). Because yield strain was approximated as the failure strain criteria, the linear part of the stress–strain curve was used to calculate strain for HDPE pipelines in this study. The loading was calculated using the same methodology used for continuous pipelines given in ASCE (1984).

Axial Strain. The axial strain was evaluated using two different scenarios, depending on the length of the PGD zone and actual ground movement. The minimum of the two strains WAs taken as the limiting axial strain. The two cases are as follows:

1. The ground movement is large, and the length of PGD zone determines the pipe strain (ε_a)

$$\varepsilon_a = \frac{t_u L}{2\pi DtE} \tag{12}$$

where $t_u = \pi Dc\alpha + \pi DH\bar{\gamma}[(1 + K0)/2]\tan\delta^1$; t_u = axial soil pressure per unit length of pipe; c = coefficient of cohesion (30 kPa); α = adhesion factor; γ = effective unit weight of soil (18 kN/m^3); and $K0$ = coefficient of soil pressure at rest.

2. Pipe strain is controlled by the amount of ground deformation instead of by the length of the PGD zone. First, the effective length of the pipeline is calculated. This is considered as the length over which the friction force acts. Effective length (L_e) is calculated using the following relation:

$$\delta_{\text{design}} = \frac{t_u L_e^2}{\pi Dt} \tag{13}$$

Strain (ε_a) is calculated using the effective length

$$\varepsilon_a = \frac{t_u L_e}{2\pi DtE} \tag{14}$$

Transverse Strain.

1. Strain is determined by the maximum PGD

$$\varepsilon_t = \pm\frac{\pi D\delta^t\text{design}}{W^2} \tag{15}$$

2. Strain is determined by the maximum resistance of the soil

$$\varepsilon_t = \pm\frac{P_u W^2}{3\pi EtD^2} \tag{16}$$

where P_u and W = maximum transverse resistance of soil and width of lateral movement (PGD), respectively. The transverse resistance of the soil (P_u) was calculated using the following relation:

$$P_u = N_{ch} cD + N_{qh} \bar{\gamma} HD \tag{17}$$

where N_{ch} = bearing capacity of clay in horizontal direction

$$N_{ch} = a + bx + \frac{c}{(x+1)^2} + \frac{d}{(x+1)^3} \tag{18}$$

where $x = H/d$ = ratio of cover depth to diameter; $a = 6.752$; $b = 0.065$; $c = -11.063$; $d = 7.119$; N_{qh} = bearing capacity factor of sandy soil in horizontal direction, where $N_{qh} = a + bx + cx^2 + dx^3 + ex^4$, where $x = H/d$, $a = 5.465$; $b = 1.548$, $c = -0.1118$, $d = 5.625 \times 10^{-3}$, and $e = -1.2227 \times 10^{-4}$.

Strain due to Buoyancy. A bending strain (ε_b) is applied to a pipe due to uplift force in the case of liquefaction. The buoyant force (F_b) acting on unit length of the pipe is

$$F_b = \frac{\pi D^2}{4}(\gamma_{\text{sat}} - \gamma_{\text{gas}}) - \pi D t \gamma_{\text{HDPE}} \tag{19}$$

where γ_{sat}, γ_{gas}, and γ_{HDPE} = unit weight of saturated soil, gas, and HDPE, respectively; and t = thickness of pipe.

The strain due to the uplift force is approximated as

$$\varepsilon_b = \pm \frac{F_b L_l^2}{3\pi E t D^2} \tag{20}$$

where L_l = length of pipe in liquefaction zone.

The resulting strain was calculated as

$$\varepsilon = \max(\varepsilon_a, \varepsilon_t, \varepsilon_b) \tag{21}$$

It was assumed that the load acts only in one direction, i.e., only transverse or only longitudinal force acts on the pipe. Because buoyancy acts only upward, it was supposed to be acting only in the cases in which it was significantly larger than transverse strain. The probability of failure was approximated as the ratio of calculated strain to critical strain

$$P_f = \frac{\varepsilon}{\varepsilon_{cr}} \tag{22}$$

Strain at yield is considered to be 15% for HDPE (Crompton 2012). The value of critical strain was determined to be 10% considering a factor of safety of 1.5. According to O'Rourke et al. (2008), this value of critical strain lies in the inelastic range, but this still is significantly below the strain at pipe rupture. Pneumatic pipe bursting, a trenchless pipe installation method, was considered as the method for pipe replacement following the guidelines in the ASCE manual of pipe bursting (Najafi 2007).

Optimal Rehabilitation Planning

A genetic algorithm–based multiobjective optimization was performed to minimize the cost of rehabilitation and maximize the seismic reliability of the network. Different alternatives were discussed in this study which can be used to rehabilitate the pipelines. The choice of the rehabilitation alternative for each pipeline is considered as the variable in the optimization framework.

The cost of pipeline network rehabilitation using CIPL lining was obtained from a leading company that has expertise in CIPL installations. The data received from the firm were used to develop a cost model using linear interpolation

$$\text{cost}(\$) = [13.598 \cdot \text{diameter (in.)} + 65] \cdot \text{length (ft)} \tag{23}$$

The cost of pipe bursting for gas pipelines was developed based on the data for pipe bursting of water mains and on insight from industry experts (Hashemi et al. 2011; Simicevic and Sterling 2003). Two different models were considered for the cost of pipe bursting. The first cost model (CM1) assumed the same cost for gas pipelines and water mains, and the second cost-estimation model (CM2) assumed an additional 25% cost in the case of pipe bursting for gas pipelines. The additional cost in the second model (CM2) was intended for managing the potential risks and more-stringent regulations for gas pipelines. The models are as follows:

$$\text{CM1: cost}(\$) = [9.5175 \cdot \text{diameter (in.)} + 4.675] \cdot \text{length (ft)} \tag{24}$$

$$\text{CM2: cost}(\$) = 1.25 \cdot [9.5175 \cdot \text{diameter (in.)} + 4.675] \cdot \text{length (ft)} \tag{25}$$

These costs are inclusive of material cost, labor cost, and other construction costs during the network rehabilitation. They do not include any aspect of operation and maintenance costs. All the costs were adjusted for inflation, and all the monetary values were expressed using the value of US dollars ($) in the year 2020 (US Bureau of Labor Statistics 2020). The constraints used in the optimization were:

- cost ≤ budget; and
- reliability postrehabilitation ≥ RI_0 (reliability index of the existing network).

The overall methodology is summarized in Fig. 4.

Demonstration

The complete framework was demonstrated for the designed representative network shown in Fig. 1. The network was expected to serve more demand in the aftermath of a seismic event after the pipelines were rehabilitated using either of the alternatives: CIPL, and replacing the aging pipes with new HDPE pipelines. Replacement of the pipelines also gives an opportunity to install pipes of larger diameter. Installation of larger-diameter pipelines can be important for two main reasons—larger pipes help to accommodate increased demand for gas in the future, and larger-diameter pipes also facilitate better hydraulic performance due to lower frictional losses. Hence, the preliminary demonstration consisted of evaluating the reliability of the network in the following four scenarios: (1) the existing network in which all the pipes are made of CI (baseline scenario), (2) CIPL of all the existing CI pipelines, (3) replacement of all the existing CI pipelines with HDPE pipelines, and (4) replacement of all the CI pipelines with a larger-diameter HDPE pipe. After the preliminary assessment, a combination of alternatives (i.e., do nothing, CIPL, or replacement with HDPE) was used for individual pipelines to maximize the network reliability at least cost.

A genetic algorithm was used to develop a multiobjective optimization framework aimed at simultaneously maximizing the seismic reliability of the network and minimizing the cost of rehabilitation. The budget was considered to be one of the constraints in the optimization framework. The following optimization parameters were considered in the multiobjective optimization:

- population size = 100;
- maximum number of generations = 25; and
- crossover fraction = 0.80.

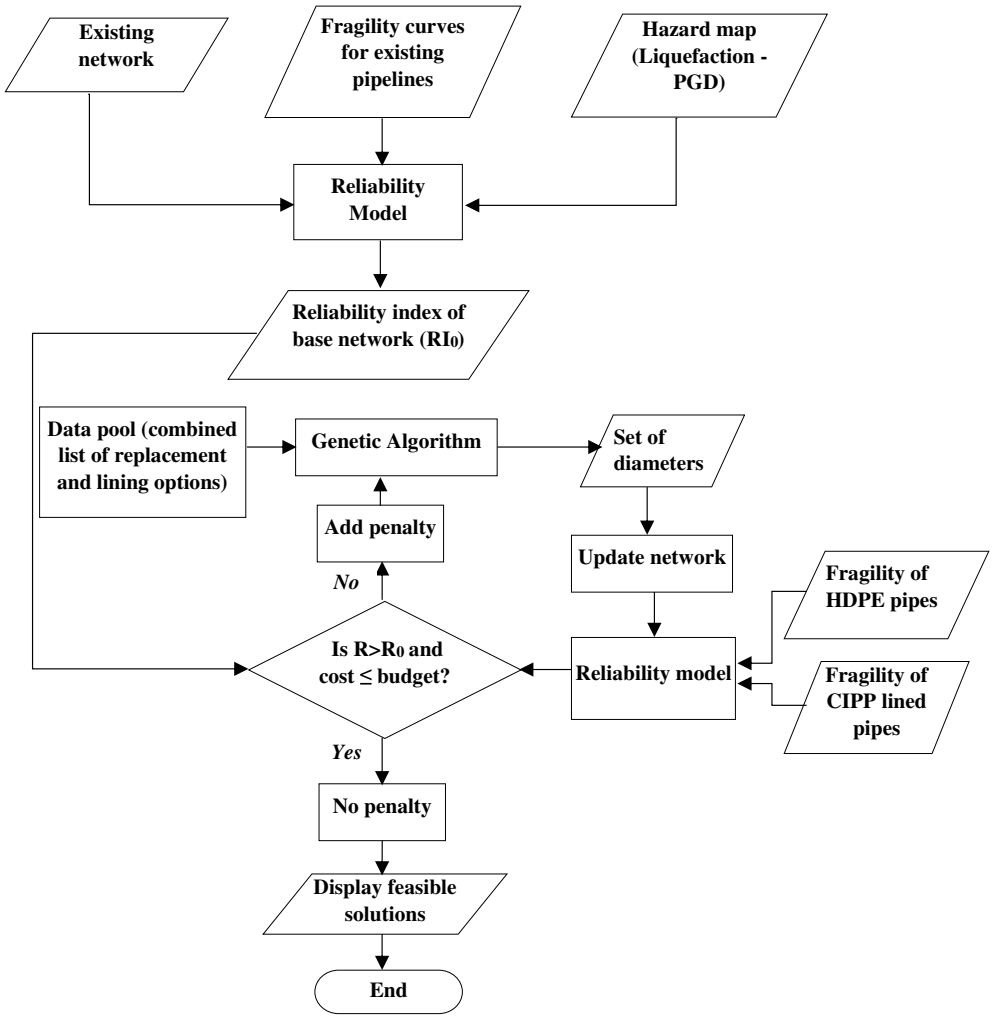

Fig. 4. Proposed optimization framework for rehabilitation planning.

Results

Reliability of Individual Scenarios

Baseline Scenario

The baseline scenario was the case in which all the pipes were made of CI and were joined using rubber gasket–type joints. Fragility curves developed by ALA (2001) were used to calculate the fragility of the pipelines. Fig. 3 shows the convergence of the reliability metric with an increasing number of random samples in Monte Carlo simulations for this scenario. The divergence was not significant after ~1,000 iterations. Therefore, N_{max} was set to 1,000 for all the simulations during optimization in this study to save computational effort. The average fragility of the pipelines was found to be 0.3699, and the system reliability index was found to be 0.1678 for the baseline scenario. Fig. 5 shows the fragilities of all the existing pipelines in the network in the form of a scatter plot.

CIPL of All Pipes

The results for the scenario involving CIPL of all the GDN pipelines are described in this section. CIPL reduced the fragility of the existing CI pipe (Fig. 6). The average fragility of CI pipes decreased from 0.3699 to 0.2867 after the application of CIPL. The reliability index of the network with all pipes lined increased from 0.1678 to 0.1862. The cost of lining all the CI pipeline with CIPL was estimated to be $62.72 million. It may be more optimal to rehabilitate fewer pipelines in the GDN using CIPL to improve seismic reliability at a reasonable cost.

Replacing All CI Pipes with HDPE Pipe of Same Size

In this alternative, all the host CI pipes were replaced with HDPE pipes of the same size. The average fragility of the pipelines after replacement with HDPE pipes of same size decreased to 0.1851 from 0.3699, and the reliability index increased to 0.2694 from 0.1678%. The cost of replacing all the CI pipeline with HDPE pipes of the same size was estimated to be $30.14 million using Cost model CM1 [Eq. (24)]. For Cost model CM2, the cost increased by a factor of 1.25, and the reliability index remained the same. Fig. 7 shows the impact of rehabilitation when only one of the four alternatives was applied to all the GDN pipelines, assuming Cost model (CM2) for replacement using the pipe bursting technique.

Figs. 6 and 7 and Table 2 give the average fragility and the average reliability of the network. Although the reliability of the network in which all pipes were replaced with HDPE was higher, this does not necessarily imply that all newer HDPE pipelines have lower fragility than CIPL-lined pipes, because the fragility improvement depends on a number of hazard and pipeline characteristics. For example, there are 144 pipelines (of 443) in which

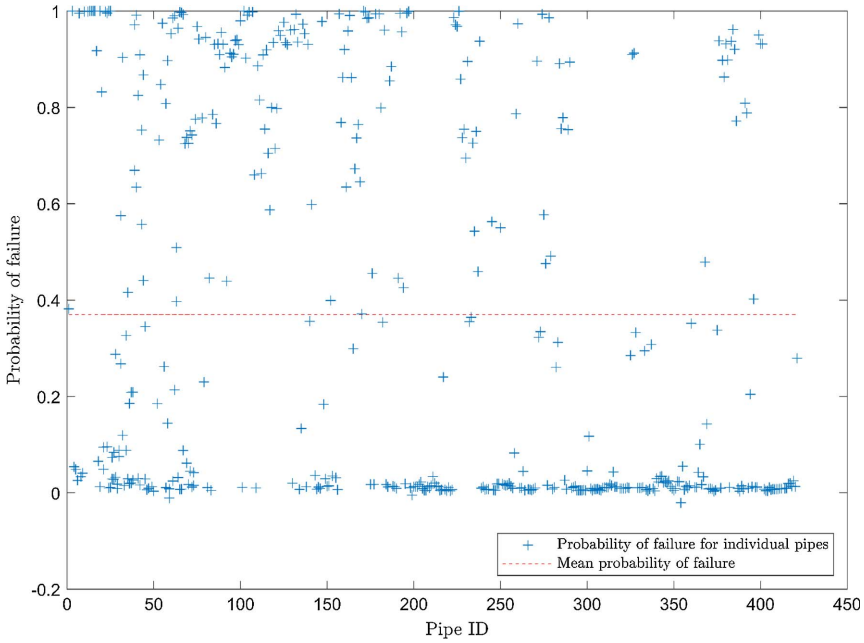

Fig. 5. Fragility of existing unlined CI pipes.

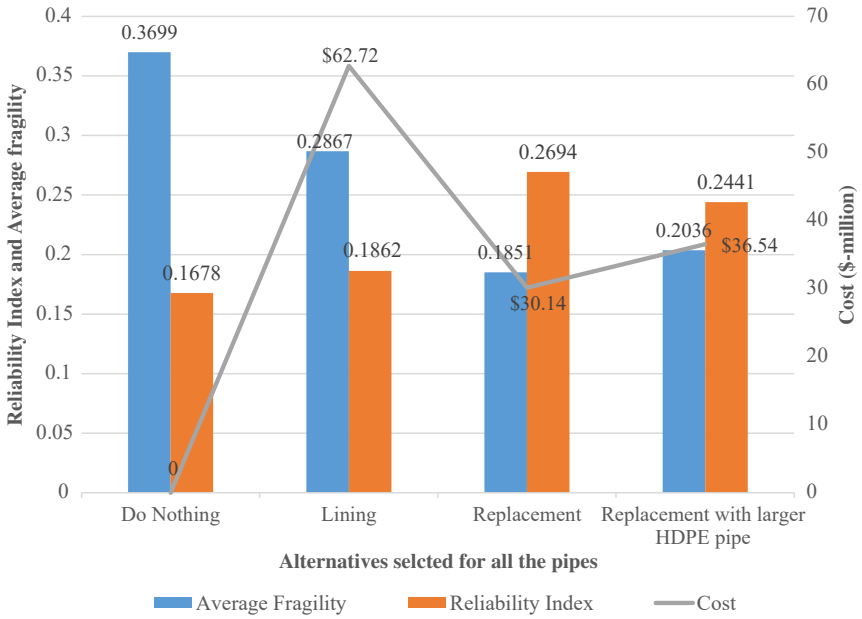

Fig. 6. Average fragility, reliability, and cost of different renewal scenarios assuming Cost model CM1 for replacement.

CIPL would lead to lower fragility compared with that of HDPE pipes. Therefore, choosing the most appropriate rehabilitation technique for each pipeline using an optimization algorithm will lead to greatest seismic reliability improvement for the GDN at the lowest cost.

Replacing All Pipes with HDPE Pipe of Larger Diameter

Larger-diameter pipelines have less pressure drop across the pipeline when the other variables remain the same [Eq. (2)]. Therefore, large-diameter pipelines may be expected to improve the reliability of the network. In addition, larger-diameter pipelines may help to cope with future demand increments. Therefore the reliability of the network was investigated with larger-diameter HDPE pipes. However, this alternative was outperformed by the previous scenario, in which all the CI pipes were replaced with the same diameter HDPE pipes. The likely reason for the poor performance of the network with larger-diameter HDPE pipelines is the increment in the seismic load during liquefaction on larger-diameter pipes, which had a detrimental impact on most of the pipelines. In addition, the cost of replacement was greater for larger-diameter pipelines. The results of all the scenarios considering only one alternative for all the pipes are summarized in Table 2. Alternative 4 was more expensive than Alternative 3, and it did not improve reliability (Figs. 6 and 7).

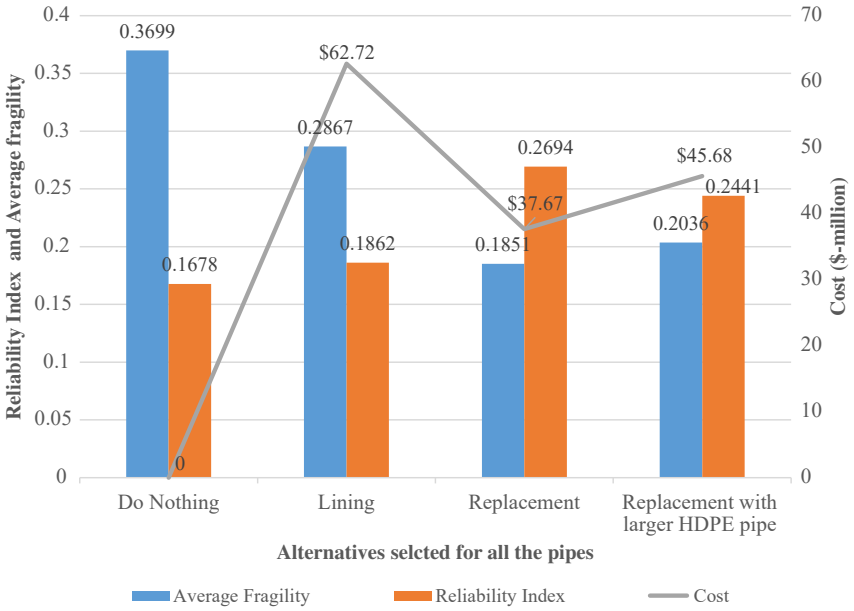

Fig. 7. Average fragility, reliability, and cost of different renewal scenarios assuming Cost model CM2 for replacement.

Table 2. Summary of results using only one rehabilitation alternative for all GDN pipelines

Rehabilitation alternatives	Alternative description	Mean of P_f	Reliability index (RI)	Cost ($ million)
Baseline scenario	Unlined CI pipelines	0.3699	0.168	0
Scenario 2	All pipelines lined with CIPL	0.2867	0.186	62.72
Scenario 3 (CM1)	All pipelines replaced with HDPE same size	0.1851	0.269	30.14
Scenario 3 (CM2)	All pipelines replaced with HDPE same size	0.1851	0.269	37.67
Scenario 4 (CM1)	All pipelines replaced with HDPE with upsizing	0.2036	0.244	36.54
Scenario 4 (CM2)	All pipelines replaced with HDPE with upsizing	0.2036	0.244	45.68

Results of Optimization Demonstration

Genetic algorithm–based multi-objective optimization was performed considering the reliability index (RI) and the cost of rehabilitation as the two objectives. The total number of variables in the optimization was 443, which was the number of pipes in the network. These variables can assume any of the available rehabilitation alternatives for individual pipes. The four alternatives considered in the optimization framework were

- Alternative 1: no rehabilitation of the individual pipeline;
- Alternative 2: CIPL of the individual pipeline;
- Alternative 3: replacement of the existing CI pipeline with HDPE pipe of the same diameter; and
- Alternative 4: replacement of the existing CI pipeline with HDPE pipe of a larger diameter.

Although Alternative 4 was considered in the optimization framework, it was not selected by the algorithm for any of the GDN pipelines because of its greater cost and inability to improve seismic reliability, which also was observed in the results presented in the previous section.

Constraints used in the optimization were

- $RI \geq RI_0$; and
- Total cost of rehabilitation $\leq$\$45 million.

Here, RI_0 is the reliability of the GDN in the baseline scenario, i.e., the reliability of the existing network in which all the pipelines are made of CI. Without any rehabilitation, the reliability of the network (RI_0) was 0.1678 (Table 2). The optimization framework rules out all potential solutions which offer a reliability index lower than that in the existing network. Similarly, the constraint on the cost is used to reject very expensive solutions. The optimization framework was demonstrated for both cost models, CM1 and CM2 [Eqs. (24) and (25), respectively]. The results from the optimization are presented as a Pareto-optimal front in Figs. 8 and 9 for Cost models CM1 and CM2, respectively.

The Pareto-optimal front presents nondominant solutions obtained in the multiobjective optimization. Four different solutions were selected from the Pareto-optimal front (Figs. 8 and 9, circled) to discuss the range of optimal rehabilitation plans. Results of the four selected optimization solutions from both the Pareto optimal fronts are shown in the form of histograms in Figs. 10 and 11 for Cost models CM1 and CM2, respectively.

Each histogram shows a combination of pipes to be left without any intervention, to be lined, and to be replaced with HDPE pipe of same size. For example, Fig. 11(a) comprises 132 pipes that were selected for CIPL, 295 pipes selected for replacement with the same-diameter HDPE pipes, and 16 pipes selected to be left without any intervention using Cost model CM2. Results corresponding to the selected scenarios are summarized in Tables 3 and 4. The results of the scenario from the Pareto-optimal front of Cost model CM2 presented in Fig. 11(a) are illustrated in Fig. 12 as an example. The map shows different alternatives suggested for all the pipelines in the GDN.

Discussion

The methodology in this study integrated various tools to develop a comprehensive framework for optimal rehabilitation planning of

J. Pipeline Syst. Eng. Pract., 2021, 12(3): 04021012

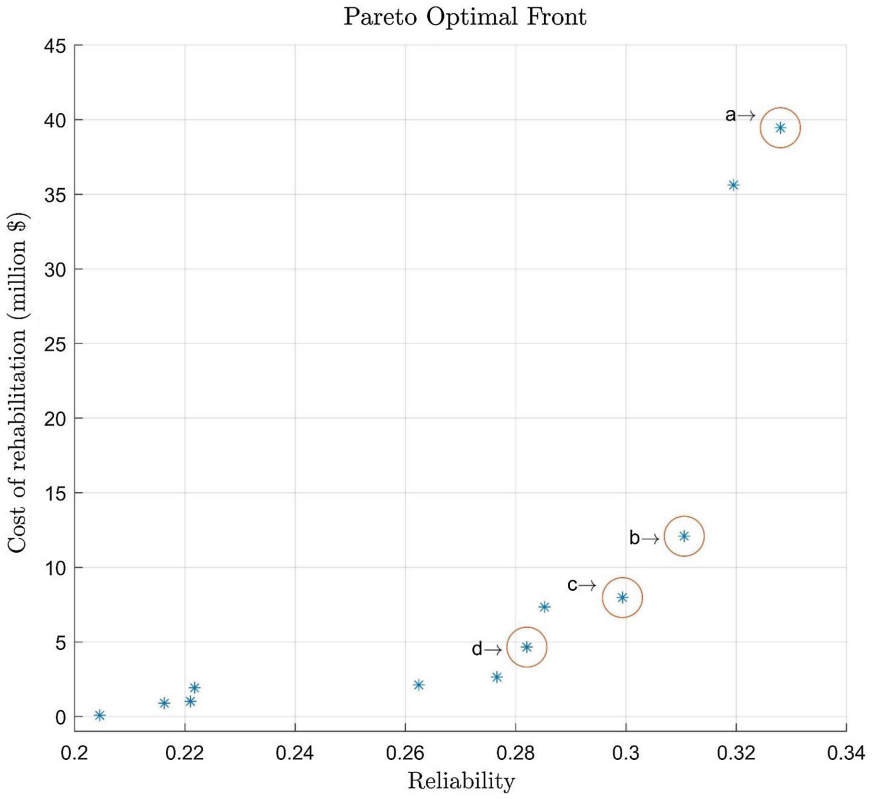

Fig. 8. Pareto-optimal solution front for multiobjective optimization for Cost model CM1.

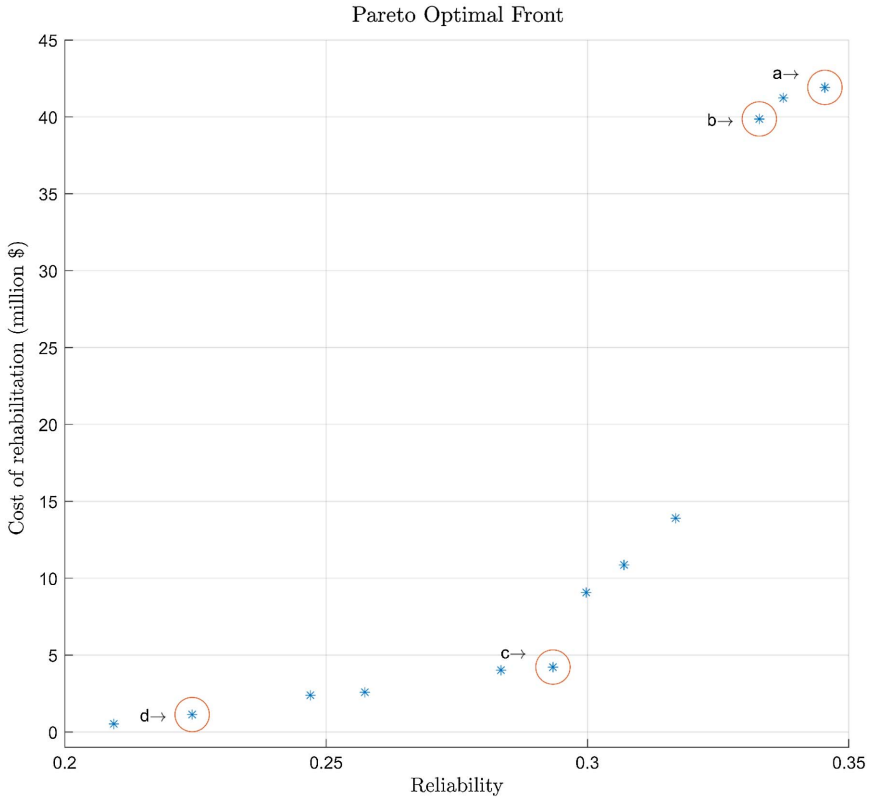

Fig. 9. Pareto-optimal solution front for multiobjective optimization for Cost model CM2.

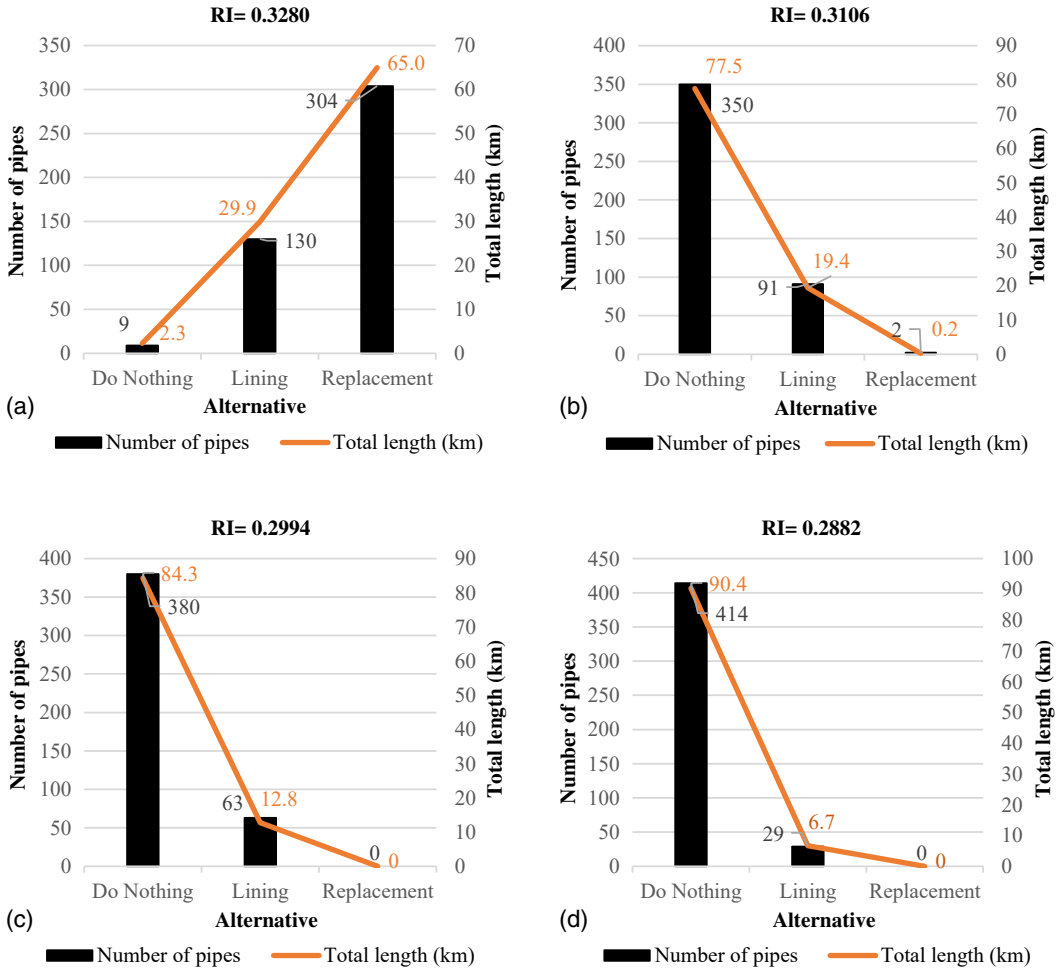

Fig. 10. Summary of selected solutions from the Pareto-optimal front for cost model CM1 (Table 3) for: (a) Scenario-A; (b) Scenario-B; (c) Scenario-C; and (d) Scenario-D.

gas distribution pipelines considering seismic reliability goals. The different tools include a flow-simulation model, a probabilistic model for pipeline failure assessment, a genetic algorithm-based optimization model, and simple analytical models for load calculations. Due to the integration of different types of models, the framework can be characterized as a hybrid approach toward seismic reliability assessment of gas distribution pipelines.

The results presented in the previous section showed that the reliability of the network can be enhanced by using either of the rehabilitation alternatives considered therein (Table 2 and Figs. 6 and 7). CIPL improves the capability of the pipelines to withstand higher axial strain due to the flexibility introduced by the liner. HDPE pipelines a perform even better in the case of large PGDs in liquefaction-prone areas (Table 2). Replacing vulnerable pipelines with larger-diameter HDPE pipelines did not produce any improvement in the system reliability due to the fact that the hazard impact also became more severe with larger HDPE pipelines.

Choosing the same rehabilitation alternative for all the pipelines (Table 2 and Figs. 6 and 7) did not necessarily provide the optimal solution. Results from the optimization scheme showed that a more reliable network can be obtained even if some of the pipelines are left as they are (Table 3 and Figs. 10 and 11). This highlights the fact that all the pipelines in the network do not have the same significance in terms of how much they contribute to the functioning of the network and to service reliability. Because the hazard has a high degree of spatial variation, it would not be straightforward to predict the impact of different rehabilitation alternatives on the network reliability improvement. The optimization algorithm considers the location of the pipeline, its vulnerability to PGD hazards, its contribution to the system operations, and the cost of its rehabilitation before deciding how each pipeline should be rehabilitated, and therein lies the value of this framework.

Some recommendations for practitioners can be made from this study. Firstly, risk hazards should be analyzed in a comprehensive manner to account for different failure modes; for example, liquefaction had remarkable spatial variation in this case. Due to this spatial variation, the modes of failure also may be different for different pipelines in a complex network. As the complexity in the characteristic of the hazard increases, it becomes harder to quantify the performance of the network accurately for the given hazard. The assessment of a wide range of hazards helps in predicting the status of the network more correctly. Furthermore, the uncertainty associated with how a buried pipeline responds to a given hazard severity is another important consideration in reliability assessment schemes. That uncertainty was addressed in this study using the Monte Carlo simulation method.

Secondly, rehabilitation need not be limited to the regular operation and upgradation of the infrastructure in general; rather, it can be used as an opportunity to make aging infrastructure more robust to extreme hazards. Another recommendation for practitioners is to prioritize the optimization of rehabilitation planning considering

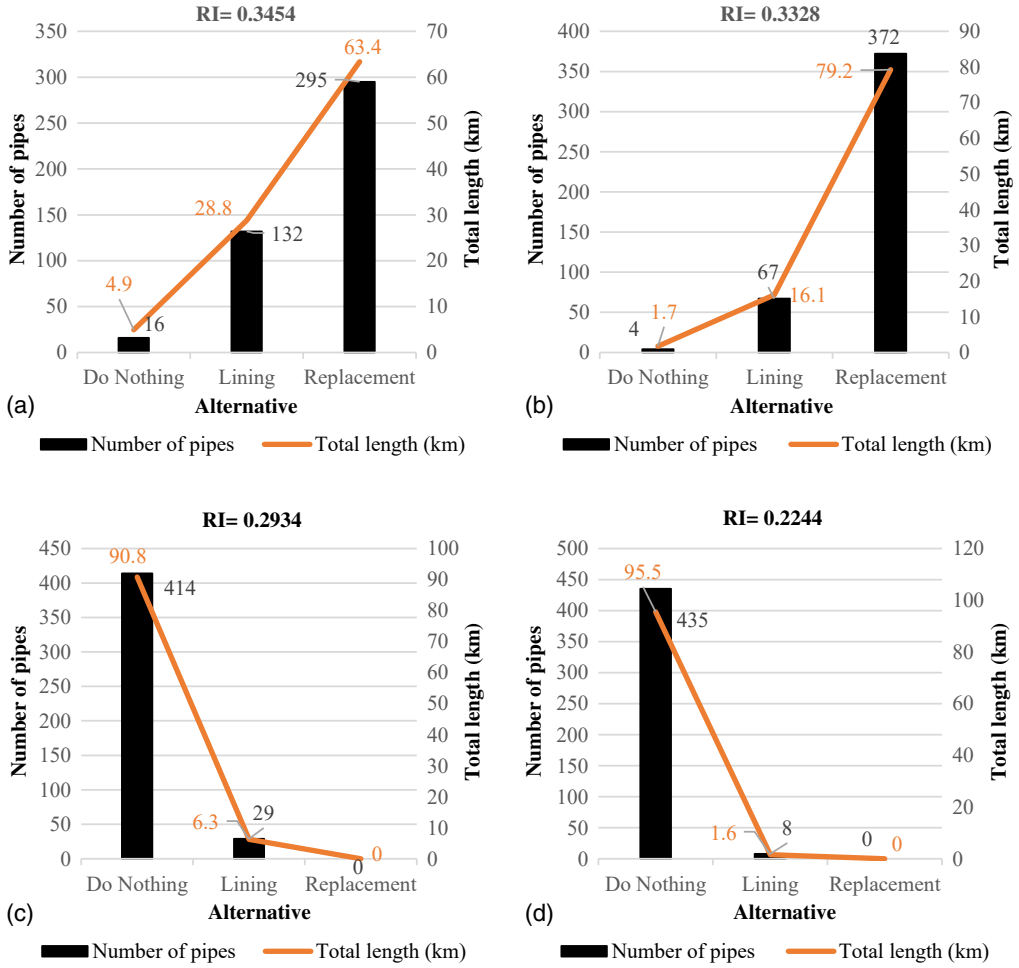

Fig. 11. Summary of selected solutions from the Pareto-optimal front for cost model CM2 (Table 4) for: (a) Scenario-A; (b) Scenario-B; (c) Scenario-C; and (d) Scenario-D.

Table 3. Results for selected Pareto-optimal solutions using Cost model CM1

Selection solutions	Reliability index	Cost ($ million)
Scenario A	0.328	39.45
Scenario B	0.310	12.08
Scenario C	0.299	7.97
Scenario D	0.282	4.65

Table 4. Results for selected Pareto-optimal solutions using Cost model CM2

Selection solutions	Reliability index	Cost ($ million)
Scenario A	0.345	34.54
Scenario B	0.333	39.86
Scenario C	0.293	4.22
Scenario D	0.224	1.12

all possible alternatives and constraints. The optimization results presented in this study may need to be adapted appropriately considering practical aspects such as contractor availability, utility preferences for pipeline choice, local codes, standards, more accurate costs, and so forth. Several other optimization algorithms along with the one used in this study can be implemented in rehabilitation projects.

Limitations and Future Direction of Research

This study considered a specific seismic event that resembled the 1886 Charleston earthquake, which is considered to be a 550-year return period event by Petersen et al. (2008). Therefore, the outcomes of this study might not reflect the impact of earthquakes which have significantly different intensity measures. Nevertheless, the approach and the optimization scheme can be adapted to any type of seismic event for which hazard maps are available and fragility equations were previously developed. A liquefaction potential map, which is an integral input of this model, commonly is not available for most regions in the US. The map used in this study was developed by Hayati and Andrus (2008) based on a series of field tests conducted across the peninsular region of Charleston city and a comprehensive review of first-hand damage records. Therefore, a prerequisite for using this model in another region is a liquefaction potential map categorizing different areas based on the different susceptibilities to liquefaction.

Different fragility functions were used for different pipeline material/liner alternatives considered in this study. The fragility of CI pipes was evaluated using the ALA fragility curves and HDPE was analyzed using simple analytical relations available for

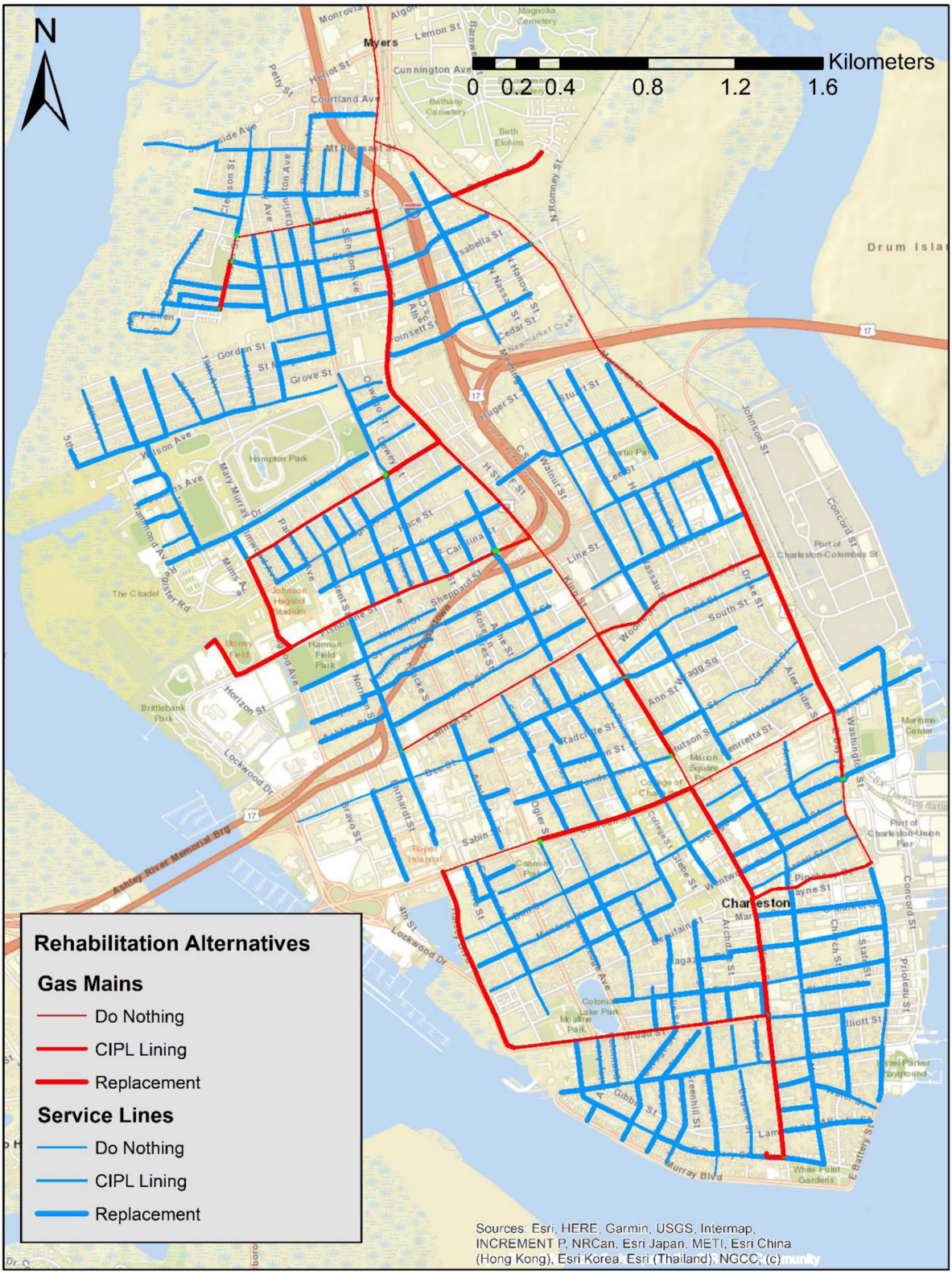

Fig. 12. GDN pipeline renewal choices for scenario in Fig. 11(a) in the Pareto-optimal front for Cost model CM2. [Base map by Esri, HERE, Garmin, USGS, Intermap, INCREMENT P, NRCan, Esri Japan, METI, Esri China (Hong Kong), Esri Korea, Esri (Thailand), NGCC, © OpenStreetMap contributors and the GIS User Community.]

soil-pipe interaction analysis of continuous pipelines. Results from a recent study of CIPL-lined CI pipes were adopted to evaluate the fragility of lined pipes. Because of the distinct considerations used in the evaluation of fragilities, the critical pipeline parameters would be different for different materials, and this distinction needs to be considered carefully to avoid grouping all pipe materials into a single category.

Another limitation of the present study is the degree of uncertainties. Epistemic uncertainties associated with different fragility functions used in the study are high. Kongar et al. (2017) compared

the PGD values evaluated using the HAZUS model with measured liquefaction-induced PGD during the 2011 Canterbury earthquake sequence. The calculated values were found to be overpredicted compared with the observed ground displacements. A more robust model for PGD calculation may improve the accuracy of the model results.

In addition, only direct capital costs were considered in the optimization framework for different rehabilitation alternatives. Consideration of life-cycle costs would add more meaning to the work, because the design life and operations and maintenance (O&M) costs of pipelines that are CIPL lined and replaced with HDPE may be different.

Conclusions

Buried pipeline networks are highly vulnerable to earthquakes in liquefaction-prone areas. CIPL of the segmented pipelines improves the performance of the network by accommodating more axial elongation at the joints during ground movements. Replacement of CI pipes with HDPE also enhances the seismic performance of the network. Because all the pipes in the networks are not exposed to the same level of threat and do not contribute equally to the overall system performance, the overall network rehabilitation can be optimized by individually selecting the appropriate rehabilitation alternatives that will maximize the seismic reliability improvement of the network at least cost.

The demonstration of the optimization framework showed that CIPL had a significant positive impact on the performance of the network during an earthquake. Previous studies of CIPL evaluated the effects of lining on a single pipeline segment only. This study further quantified the effects of lining from a systemic point of view by combining the fragility functions with a gas-flow simulation model. HDPE was used in the natural gas distribution network as the preferred material for small-diameter pipes. HDPE also has been found to perform very well even during permanent ground movements in historical earthquakes. This study quantified the performance of HDPE pipelines subject to PGD using a simple limit-state model. The impact of using HDPE for seismic reliability-focused rehabilitation was not established quantitatively in the majority of previous studies.

The optimization framework was demonstrated for CIPL and HDPE pipelines, but the scope of this work is not limited to only these two alternatives. Other rehabilitation options can be integrated to the framework with appropriate fragility functions for those alternatives. The contribution of this study is its exploration of the potential to enhance the seismic reliability of GDNs during rehabilitation using on a genetic algorithm–based optimization framework.

Data Availability Statement

Some or all data, models, or code that support the findings of this study are available from the corresponding author upon reasonable request.

Acknowledgments

This study is supported by National Science Foundation (NSF) under Grant No. CRISP-1638321. All the views and interpretations presented in the paper are those of the authors and do not represent the views of NSF on the topics discussed herein. The authors also thank the trenchless industry professionals who provided pipeline renewal cost data for this study.

References

ALA (American Lifelines Alliance). 2001. "Seismic fragility formulations for water systems: Part 1—Guidelines." Accessed January 20, 2020. http://www.americanlifelinesalliance.com/pdf/Part_1_Guideline.pdf.

Ameri, M. R., and J. W. van de Lindt. 2019. "Seismic performance and recovery modeling of natural gas networks at the community level using building demand." *J. Perform. Constr. Facil.* 33 (4): 04019043. https://doi.org/10.1061/(ASCE)CF.1943-5509.0001315.

Argyrou, C., D. Bouziou, T. D. O'Rourke, and H. E. Stewart. 2018. "Retrofitting pipelines with cured-in-place linings for earthquake-induced ground deformations." *Soil Dyn. Earthquake Eng.* 115 (Dec): 156–168. https://doi.org/10.1016/j.soildyn.2018.07.015.

ASCE. 1984. *Guidelines for the seismic design of oil and gas pipeline systems*, 473–473. Reston, VA: ASCE.

Ayala, A. G., and M. J. O'Rourke. 1989. "Effects of the 1985 Michoacan earthquake on water systems and other buried lifelines in Mexico." Accessed January 20, 2020. https://nehrpsearch.nist.gov/static/files/NSF/PB89207229.pdf.

Ayala H, L. F., and C. Y. Leong. 2013. "A robust linear-pressure analog for the analysis of natural gas transportation networks." *J. Nat. Gas Sci. Eng.* 14 (Sep): 174–184. https://doi.org/10.1016/j.jngse.2013.06.008.

Chenna, R., A. Singh, K. Mohan, and P. Ramcharla. 2014. "Vulnerability assessment of buried pipelines: A case study." *Front. Geotech. Eng.* 3 (1): 24–33.

Cret, L., F. Yamazaki, S. Nagata, and T. Katayama. 1993. "Earthquake damage estimation and decision analysis for emergency shut-off of city gas networks using fuzzy set theory." *Struct. Saf.* 12 (1): 1–19. https://doi.org/10.1016/0167-4730(93)90015-S.

Crompton, T. R. 2012. "Mechanical properties of polymers." Chap. 1 in *Physical testing of plastics*, 1–125. Shropshire, UK: Smithers Rapra Technology.

Dominion Energy. 2018. "Operational capacity report. Dominion energy Carolina gas transmission, LLC." Accessed January 10, 2019. https://ebb.dominionenergy.com/InformationalPostings/Capacity/OperAvail.aspx.

Elhmadi, K., and M. J. O'Rourke. 1990. "Seismic damage to segmented buried pipelines." *Earthquake Eng. Struct. Dyn.* 19 (4): 529–539. https://doi.org/10.1002/eqe.4290190405.

Elton, D. J., and T. Hadj-Hamou. 1990. "Liquefaction potential map for Charleston, South Carolina." *J. Geotech. Eng.* 116 (2): 244–265.

Farahmandfar, Z., K. R. Piratla, and R. D. Andrus. 2016. "Resilience evaluation of water supply networks against seismic hazards." *J. Pipeline Syst. Eng. Pract.* 8 (1): 04016014. https://doi.org/10.1061/(ASCE)PS.1949-1204.0000251.

FEMA. 2012. *Multi-hazard loss estimation methodology, earthquake model: Hazus-MH 2.1 user manual*, 863. Washington, DC: FEMA.

Hashemi, B., T. Iseley, and J. Raulston. 2011. Water pipeline renewal evaluation using AWWA Class IV CIPP, pipe bursting, and open-cut. *ICPTT 2011: Sustainable Solutions for Water, Sewer, Gas, and Oil Pipelines—Proc., of the Int. Conf. on Pipelines and Trenchless Technology 2011*, 1257–1266. Reston, VA: ASCE. https://doi.org/10.1061/41202(423)133.

Hayati, H., and R. D. Andrus. 2008. "Liquefaction potential map of Charleston, South Carolina based on the 1886 earthquake." *J. Geotech. Geoenviron. Eng.* 134 (6): 815–828. https://doi.org/10.1061/(ASCE)1090-0241(2008)134:6(815).

Housner, G. W., and P. C. Jennings. 1972. "The San Fernando California earthquake." *Earthquake Eng. Struct. Dyn.* 1 (1): 5–31. https://doi.org/10.1002/eqe.4290010103.

Iwasaki, T., T. Arakawa, and K.-I. Tokida. 1984. "Simplified procedures for assessing soil liquefaction during earthquakes." *Int. J. Soil Dyn. Earthquake Eng.* 3 (1): 49–58. https://doi.org/10.1016/0261-7277(84)90027-5.

Kongar, I., S. Giovinazzi, and T. Rossetto. 2017. "Seismic performance of buried electrical cables: evidence-based repair rates and fragility

functions." *Bull. Earthquake Eng.* 15 (7): 3151–3181. https://doi.org/10.1007/s10518-016-0077-3.

Liu, D., W. Zhou, and S. He. 2017. "Risk assessment for urban gas transmission and distribution system using fuzzy comprehensive evaluation method." *J. Pipeline Syst. Eng. Pract.* 9 (1): 04017038. https://doi.org/10.1061/(ASCE)PS.1949-1204.0000307.

Liu, W., Z. Li, Z. Song, and J. Li. 2018. "Seismic reliability evaluation of gas supply networks based on the probability density evolution method." *Struct. Saf.* 70: 21–34. https://doi.org/10.1016/j.strusafe.2017.10.001.

Miao, H., W. Liu, C. Wang, and J. Li. 2016. "Artificial earthquake test of gas supply networks." *Soil Dyn. Earthquake Eng.* 90 (Feb): 510–520. https://doi.org/10.1016/j.soildyn.2016.09.022.

Najafi, M. 2007. *Pipe bursting projects: ASCE manuals and reports on engineering practice No. 112*. Reston, VA: ASCE.

Nakai, K., and T. Yokoyama. 2015. "Uniaxial compressive response and constitutive modeling of selected polymers over a wide range of strain rates." *J. Dyn. Behav. Mater.* 1 (1): 15–27. https://doi.org/10.1007/s40870-015-0003-9.

Netravali, A. N., T. D. O'Rourke, S. Shaw, and T. Bond. 2003. *Evaluation of Starline 2000-PSE cured-in-place lining system for cast iron gas distribution pipelines*. Rep. Contract No. 39802. New York: New York Gas Group.

Nuti, C., A. Rasulo, and I. Vanzi. 2010. "Seismic safety of network structures and infrastructures." *Struct. Infrastruct. Eng.* 6 (1–2): 95–110. https://doi.org/10.1080/15732470802663813.

O'Rourke, M., and C. Nordberg. 1992. "Behavior of buried pipelines subject to permanent ground deformation." Accessed July 19–24, 1992. http://www.iitk.ac.in/nicee/wcee/article/10_vol9_5411.pdf.

O'Rourke, T. D., J. M. Jezerski, N. A. Olson, A. L. Bonneau, M. C. Palmer, H. E. Stewart, M. J. O'rourke, and T. Abdoun. 2008. "Geotechnics of pipeline system response to earthquakes." In *Proc., Geotechnical Earthquake Engineering and Soil Dynamics IV*, 1–38. Reston, VA: ASCE. https://doi.org/10.1061/40975(318)193.

Petersen, M. D., A. D. Frankel, S. C. Harmsen, C. S. Mueller, K. M. Haller, R. L. Wheeler, and K. S. Rukstales. 2008. "Documentation for the 2008 update of the United States National Seismic Hazard Maps." Accessed February 10, 2021. https://pubs.usgs.gov/of/2008/1128/ofr20081128v1.1.pdf.

Poljanšek, K., F. Bono, and E. Gutiérrez. 2012. "Seismic risk assessment of interdependent critical infrastructure systems: The case of European gas and electricity networks." *Earthquake Eng. Struct. Dyn.* 41 (1): 61–79. https://doi.org/10.1002/eqe.1118.

Praks, P., V. Kopustinskas, and M. Masera. 2017. "Monte-Carlo-based reliability and vulnerability assessment of a natural gas transmission system due to random network component failures." *Sustainable Resilient Infrastruct.* 2 (3): 97–107. https://doi.org/10.1080/23789689.2017.1294881.

Prasad, V., K. R. Piratla, B. Caswell, and S. Banerjee. 2020. "Seismic reliability evaluation of city-level gas distribution networks using flow-based simulation modeling." In *Proc., Construction Research Congress 2020: Infrastructure Systems and Sustainability*, 390–398. Reston, VA: ASCE.

Psyrras, N. K., and A. G. Sextos. 2018. "Safety of buried steel natural gas pipelines under earthquake-induced ground shaking: A review." *Soil Dyn. Earthquake Eng.* 106: 254–277. https://doi.org/10.1016/J.SOILDYN.2017.12.020.

Ramberg, W., and W. Osgood. 1943. "Description of stress-strain curves by three parameters." Accessed January 20, 2020. https://ntrs.nasa.gov/search.jsp?R=19930081614.

Scawthorn, C., M. Miyajima, Y. Ono, J. Kiyono, and M. Hamada. 2006. "Lifeline aspects of the 2004 Niigata Ken Chuetsu, Japan, earthquake." Supplement, *Earthquake Spectra* 22 (1): 89–110. https://doi.org/10.1193/1.2173932.

Simicevic, J., and R. Sterling. 2003. "Survey of bid prices for trenchless methods." Accessed August 4, 2020. http://library.ttcils.latech.edu/cgi-bin/koha/opac-detail.pl?biblionumber=17979&query_desc=kw%2Cwrdl%3A.

Singhal, A. C., and J. C. Benavides. 1983. "Axial and bending behavior of pipeline joints." Accessed August 4, 2020. https://www.jstor.org/stable/pdf/41272928.pdf?refreqid=excelsior%3Ad8f2b908b0c9a984c824100bba9b96d5.

Stern, R. E., J. Song, and D. B. Work. 2017. "Accelerated Monte Carlo system reliability analysis through machine-learning-based surrogate models of network connectivity." *Reliab. Eng. Syst. Saf.* 164 (Aug): 1–9. https://doi.org/10.1016/J.RESS.2017.01.021.

Stewart, H. E., T. D. O'rourke, B. P. Wham, A. N. Netravali, C. Argyrou, and X. Zeng. 2015. *Performance testing of field-aged cured-in-place liners (CIPL) for cast iron piping: Final report*. Ithaca, NY: Cornell Univ.

Tchórzewska-Cieślak, B., K. Pietrucha-Urbanik, M. Urbanik, and J. R. Rak. 2018. "Approaches for safety analysis of gas-pipeline functionality in terms of failure occurrence: A case study." *Energies* 11 (6): 1589. https://doi.org/10.3390/en11061589.

US Bureau of Labor Statistics. 2020. "CPI inflation calculator." Accessed July 17, 2020. https://www.bls.gov/data/inflation_calculator.htm.

Yiğit, A., M. A. Lav, and A. Gedikli. 2017. "Vulnerability of natural gas pipelines under earthquake effects." *J. Pipeline Syst. Eng. Pract.* 9 (1): 04017036. https://doi.org/10.1061/(asce)ps.1949-1204.0000295.